Synthesis And Characterization Of Lanthanum Doped Mg-Zn Ferrite Nanoparticles Prepared by SOL-GEL Method

R. U. Mullai[1], P. Priyadharsini Pradeep[2], G. Chandrasekaran[*]

[*]Department of physics, School of Physical, Chemical and Applied Sciences, Pondicherry University, Pondicherry 605014, INDIA.

[1-2]Department of Physics, Government Arts College, Thiruvannamalai-606 603.Tamil Nadu, INDIA.

Corresponding Address:

muhairu@gmail.com

Research Article

Abstract: The Ferrite compositions of La substituted $Mg_{0.5}Zn_{0.5}La_xFe_{2-x}O_4$ (x=0.0, 0.025, 0.05, 0.075, 0.1) are prepared using sol-gel citrate-nitrate. The as prepared powders are annealed at 600˚ c to improve structural and magnetic properties. The thermal behavior of ferrite from its gel is studied by using DSC and the structural and morphological studies of the ferrites have been investigated by using XRD, SEM-EDAX and FAR-IR respectively. The magnetic properties of the samples are studied using VSM at room temperatures. The samples are found to exhibit saturation magnetization. Lanthanum doped Mg-Zn ferrites are found to exhibit large relaxation which make them useful for microwave applications.

Key words: Magnesium-zinc ferrite; Cation distribution; Saturation magnetization; Grain Size; La dopped; Rare earth

1. Introduction

Ferrites are technologically important materials. They have been extensively investigated to extend their domain of applications in electronics. In general, ferrite materials are receiving much attention in high frequency applications such as inductors, waveguides, isolators, circulators, and phase shifters. Ferrimagnetic materials have high resistivity and anisotropic properties. Ferrites that are used in transformer or electromagnetic cores contain Nickel, Zinc or manganese compounds. They have low coercively and therefore called as soft ferrites. Because of their comparatively low losses at high frequencies, they are extensively used in the cores of Switched-Mode Power Supply (SMPS), RF transformers and inductors [1-3]. Ferrites because of their high permeability and permittivity constitute the major components of the devices that are used in the high frequency applications. A Ferrimagnetic material is one, which below a transition temperature possesses a spontaneous magnetization due to non parallel arrangement of the strongly coupled magnetic moments. Neel [4] has unrevealed the idea of ferrimagnetisms and formulated a general theory to explain it. J.L. Snoek [5] has explained the electrical and magnetic properties of ferrites which helped to improve the high frequency applications of ferrites. Immediately after, a number of scientists and engineers became involved in basic studies, manufacturing, improvement, measurement and application of ferrites. The nanostructured ferrites exhibit properties that are different from their bulk counterparts because of their extremely fine grain size. A principal effect of finite size on a magnetic particle is the breaking of exchange bonds which strongly affects the exchange interaction [6]. The magnetic properties of ferrite nanoparticles such as saturation magnetization, coercivity and ordering temperature are affected grossly with the change in particle size [7].

2. Experimental Procedure

The mixed nanoferrites of $(Mg_{0.5}Zn_{0.5})La_xFe_{2-x}O_4$ (where x = 0.0, 0.025, 0.05, 0.075 and 0.1) are prepared using sol-gel synthesis method .High quality zinc nitrate, ferric nitrate, magnesium nitrate, lanthanum nitrate and citric acid are taken according to the proposed stoichiometry ratio. Citric acid which possesses a high heat of combustion plays a role of organic fuel and it provides the platform for the redox reactions to occur between the reactants during the course of combustion. The important advantage of this method is that it dose not employ water or any other solvent for the preparation of the precursor solutions and therefore avoiding impurities caused by water completely. The metal nitrates are hygroscopic and they tend to form a slurry mixture when mixed with citric acid. The mixture is dehydrated by heating at 70˚c. The dried mixture is then subjected to a suitable closed heating mechanism which ignites a combustion process in it. Since the metal nitrates also plays the role of oxidants, the combustion process can take place effectively utilizing the oxygen content of the reactants themselves. The combustion process yields

voluminous ash accompanied by fumes. During the chemical processes expected to occur in an instantaneous moment are given as follows.

The stoichiometry condition of $(Mg_{0.5}Zn_{0.5})\ Fe_2O_4$ is ensured by means of the balanced chemical formula:

$$0.5Mg(NO_3)_2.6H_2O + 0.5Zn(NO_3)_2.6H_2O + 2Fe(NO_3)_3.9H_2O \longrightarrow Mg_{0.5}Zn_{0.5}Fe_2O_4 + 22.5\ H_2O + 8\ NO_2\uparrow + 2O_2\uparrow \quad \text{------- (1)}$$

The data of molecular weight of metal nitrates taken for the present synthesis are

$Mg\ (NO_3)_2.6H_2O \longrightarrow$ 256.43gm.
$Zn\ (NO_3)_2\ .6H_2O \longrightarrow$ 297.48gm.
$Fe\ (NO_3)_3\ .9H_2O \longrightarrow$ 404.00gm.
$LaN_3O_9.6H_2O \longrightarrow$ 433.02 gm.

For the preparation of 10gm of $((Mg_{0.5}Zn_{0.5})\ Fe_2O_4$, the gram weight of the metal nitrate is estimated as:

0.5 $Mg\ (NO_3)_2.6H_2O$ = 5.8401gm.
0.5 $Zn\ (NO_3)_2.6H_2O$ = 6.7751gm.
2.0 $Fe\ (NO_3)_3.9H_2O$ = 36.8044gm.

When the Lanthanum is doped, the stoichiometry condition of $(Mg_{0.5}Zn_{0.5})\ LaxFe2_{-x}O_4$ is ensured by means of the following balanced chemical formula:

$$0.5Mg(NO_3)_2.6H_2O + 0.5Zn(NO_3)_2.6H_2O + 0.025LaN_3O_9.6\ H_2O + 1.975Fe(NO_3)_3.9H_2O \longrightarrow La_{0.025}\ Mg_{0.5}Zn_{0.5}Fe_{1.975}O_4 + 23.93\ H_2O + 8\ NO_2 + 4O_2 \text{ ------(2)}$$

For the preparation of 10gm of $(Mg_{0.5}Z\ n_{0.5})$ $La_{0.025}Fe_{1.975}O_4$, the gram weight of the metal nitrate is estimated as:

$0.025LaN_3O_9.6H_2O$ = 0.4878 gm.
$0.5Mg\ (NO_3)_2.6H_2O$ = 5.7773gm.
$0.5Zn\ (NO_3)_2\ .6H_2O$ = 6.7022gm.
$1.975Fe\ (NO_3)_3\ .9H_2O$ = 35.9533gm.

The expected chemical reactions during the three stages of heat treatment are: sol-gel preparation by mixing of solutions:

At 100˚c: removal of H_2O

$$LaN_3O_9 + Mg(NO_3)_2.6H_2O + Zn(NO_3)_2.6H_2O + Fe(NO_3)_3.9H_2O + C_6H_8O_7 \longrightarrow LaN_3O_9 + Mg(NO_3)_2 + Zn(NO_3)_2 + Fe(NO_3)_3 + H_2O\uparrow$$

At 350˚c liberation of NO_2

$$LaN_3O_9 + Mg\ (NO_3)_2 + Zn(NO_3)_2 + Fe\ (NO_3)_3 \longrightarrow LaO + MgO + ZnO + Fe_2O_3 + NO_2 \quad \text{------ (3)}$$

Due to the above two stages, heat released may mount up to create a temperature of 1000 °C which is sufficient for the formation and subsequent crystallization of the desired product

$$0.025LaO + 0.5MgO + 0.5ZnO + 0.9875Fe_2O_3 \longrightarrow Mg_{0.5}Zn_{0.5}La_{0.025}Fe_{1.975}O_4\text{----- (4)}$$

Ultra fine ferrite particles are obtained and made ready for characterization.

The product is gently crushed into a fine powder using the mortar and pestle. The as-synthesized powder so formed is characterized using XRD, DSC, SEM-EDAX, FAR-IR, and VSM.

3. Result and discussion

3.1Thermal analysis of dried gel precursor

The DSC (Differential Scanning Calorimetric) curves observed for dried gel precursors of $Mg_{0.5}Zn_{0.5}La_xFe_{2-x}O_4$ in the temperature range 50-500^{o}C as shown in Fig 1. It is seen from Fig.1 that there are dominate exothermic and endothermic peaks along with an array of small humps around different mean temperatures. The different peaks are explained on the basis of redox-reaction, phase formation, crystallization. The precursors for all the concentrations show a major endothermic peak in the temperature range 120-130^{o}C which can be assigned to the evaporation of water molecules over lapped with redox reactions during the formation.An intense exothermal peak in the temperature range 210-250^{o}C indicate the vigorous auto-combustion reaction of the precursor corresponding to an auto-catalytic anionic oxidation–reduction reaction between the nitrate and citrate molecules [8]. As explained in the chemical reaction mentioned in the last chapter. The sharpness of the peaks signifies that the reaction takes place in an abrupt releasing of an enormous amount of heat energy. It is noted that though the mean temperature of formation of ferrite phase is almost the same for all the samples, the heat energy released by each of them is found to vary. The maximum amount of heat energy has been let out by x = 0.0 sample i.e. the case of un-doped Mg-Zn ferrite. Thus doping $Mg_{0.5}Zn_{0.5}Fe_2O_4$ with La is co-relatable to the reduction of the intensity of the exothermic peak. It may be attributed to formation of La-O bond which requires a higher quantity of energy for its binding. As enthalpy change is directly proportional to the negative of strength of bond formed [9] an exothermic peak reducing in intensity with La doping is produced.

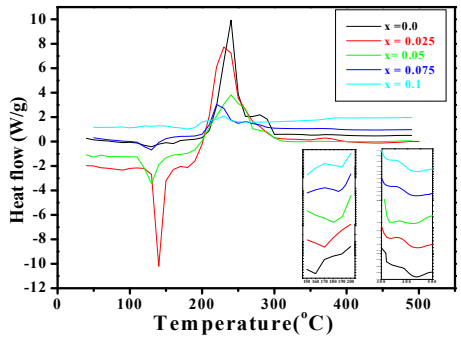

Fig.1: DSC analysis of dried gel precursors of $Mg_{0.5}Zn_{0.5}La_{2-X}O_4$

A decrease in the amount of heat created during combustion could result in a good deal of loss of quantity of energy for completing the reaction. The loss of required energy for forming the compound leads to un-doped secondary phases of oxides of La. The explanation is in good agreement with the report of XRD study of these ferrites. A small hump in the tail end of the exothermic peak around 300ºC indicates the removal of residual hydrocarbons and subsequent crystallization of the ferrite. From the above observations, it is seen that La^{3+} incorporation constrains the single phase formations prevalently. A close scrutiny of the curves indicate the presence of a weak endothermic curve around 160-200ºC which may be attributed to the magnetic transition of these ferrites. Another endothermic peak for all the samples sans x = 0.0 case is noted around 437- 450ºC which may be attributed to the magnetic transition of $LaFeO_3$. Derek Craik [10] has reported Curie temperature for bulk La ortho ferrites equal to 470ºC. The endothermic peaks reported here are too small to resolve due to other overlapped reaction mechanisms and needs confirmation through magnetic study.

3.2 Structural Study

3.2.1 XRD Study

The XRD patterns of as-prepared $Mg_{0.5}Zn_{0.5}La_xFe_{2-x}O_4$ (where x = 0.0, 0.025, 0.05, 0.075 and 0.1) are shown in Fig. 2. The XRD patterns are found to possess well resolved, sharp and intense peaks corresponding to planes (111), (220), (311), (222), (400), (422), (333) and (440). The samples are found to possess single phase for a Lanthanum concentration of x = 0.025. For higher concentrations of La, a secondary phase fitting to $LaFeO_3$ compound (JCPDS powder diffraction file No: 75-0541) [11] crops up at angles 32º, 43º and 57º as evident from the XRD patterns. It is proposed from the DSC study that the heat released during the auto-combustion reaction is insufficient for the formation of single phase ferrite. This has apparently resulted in the La ion not getting substituted in the lattice properly. Due to the larger bond energy of La^{3+}– O^{2-} as compared to that of Fe^{3+}– O^{2-}, the more energy is needed to make La^{3+} ions enter into lattice and form the bond of La^{3+}– O^{2-}. Therefore, La-substituted ferrites have higher thermal stability relative to pure ferrite, and more energy is needed for the La-substituted samples to complete crystallization and grow the grains [12] .

In practice, doping of La into the ferrite is achieved through a process of solid solution. It is seen in Fig.2 that the intensity of the secondary phase increases with the increase in La content. It implies that the substituted La^{3+} ion has a solubility limit in the spinal lattice. The degree of substitution of Fe^{3+} by La^{3+} ion depends largely on their ionic radii. Since the ionic radius of La^{3+} ions is larger compared to that of Fe^{3+} ions, the replacement of Fe^{3+} by La^{3+} is limited in the spinal lattice. Therefore when the solubility limit is reached at x = 0.025 and from x = 0.05, the redundant La^{3+} ions form $LaFeO_3$ on the grain boundaries [11, 12].

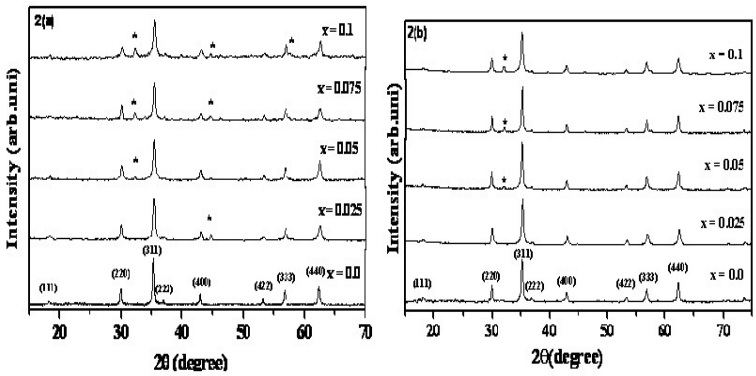

Fig.2: The XRD pattern of $Mg_{0.5}Zn_{0.5}La_{2-X}O_4$ (a) as synthesized and (b) annealed at 600ºC

The as-prepared $Mg_{0.5}Zn_{0.5}La_xFe_{2-x}O_4$ is subjected to annealing process at 600ºC for 2 hours. The annealing process has definitely helped in reducing the intensity of the secondary phases which is obvious from the XRD

patterns shown in Fig.3.The experimental and theoretical lattice constants and grain sizes of the annealed ferrite samples are obtained from the XRD data and are given in table 1. It is seen from table.1 that the lattice constant values of the ferrites increase with the substitution of La. The trend can be explained on the basis of the ionic radii of the constituent ions. The La^{3+} ions have a strong preference for octahedral site and therefore replace Fe^{3+} ions at octahedral site (B) in cube spinal lattice. This makes the lattice to expand and lattice parameter increase since radii of La^{3+} ion (0.106 nm) is bigger than that of Fe^{3+} ion (0.064 nm) [11-13]. This is in accordance with results in table 1

Table 1: Structural data obtained from XRD analysis

Conce-ntration (X)	Lattice constant(A°)		Grain size nm	Cation distribution	
	Exp	Theo		A-site	B-site
0.0	8.4271	8.4245	35	$Mg^{2+}_{0.15}Zn^{2+}_{0.45}Fe^{3+}_{0.4}La^{3+}_{0}$	$Mg^{2+}_{0.35}Zn^{2+}_{0.05}Fe^{3+}_{1.05}Fe^{2+}_{0.55}La^{3+}_{0}$
0.025	8.4345	8.4357	30	$Mg^{2+}_{0.153}Zn^{2+}_{0.425}Fe^{3+}_{0.416}La^{3+}_{0.006}$	$Mg^{2+}_{0.347}Zn^{2+}_{0.075}Fe^{3+}_{1.049}Fe^{2+}_{0.51}La^{3+}_{0.019}$
0.05	8.4423	8.4483	27	$Mg^{2+}_{0.154}Zn^{2+}_{0.418}Fe^{3+}_{0.418}La^{3+}_{0.01}$	$Mg^{2+}_{0.346}Zn^{2+}_{0.082}Fe^{3+}_{1.0485}Fe^{2+}_{0.4835}La^{3+}_{0.04}$
0.075	8.4494	8.4584	25	$Mg^{2+}_{0.155}Zn^{2+}_{0.4}Fe^{3+}_{0.422}La^{3+}_{0.023}$	$Mg^{2+}_{0.345}Zn^{2+}_{0.1}Fe^{3+}_{1.047}Fe^{2+}_{0.456}La^{3+}_{0.052}$
0.1	8.4567	8.4695	21	$Mg^{2+}_{0.156}Zn^{2+}_{0.387}Fe^{3+}_{0.424}La^{3+}_{0.033}$	$Mg^{2+}_{0.344}Zn^{2+}_{0.113}Fe^{3+}_{1.046}Fe^{2+}_{0.43}La^{3+}_{0.067}$

The grain sizes calculated using Scherer's formula is found to be well within the nano regime. It is noted that the grain sizes decrease with increasing La content, which is in agreement with the results from the literature [12-14]. It is explained to be due to the diffusion of La^{3+} ions to the grain boundaries which segregate to form the secondary phase during the heat treatment. This segregation process will inhibit the grain growth by limiting grain mobility. Using the ionic size data for the respective ions, the Cation distribution of the ferrites has been estimated theoretically with reference to their experimental lattice constant values using the following formula proposed by Bhongale et al. [8].

$$a = \frac{\left\{\left(\frac{r_a}{\sqrt{3}} + r_b + 2.0951 r_o\right) + \left[\left(\frac{r_a}{\sqrt{3}} + r_b + 2.0951 r_o\right)^2 - 1.866\left(1.333 r_a^2 + 0.0675 r_o^2 - 0.6 r_a r_o\right)\right]^{\frac{1}{2}}\right\}}{1.106} \quad \text{..... (3.1)}$$

Where r_a and r_b are the radii of the ions present in A- and B-site, respectively, where as r_o is the ionic radius of oxygen. An indigenous computer program in FORTRAN-77 has been developed to determine the cation distribution. Among the various possible distributions, the one which fits well with the experimental lattice constant value and compatible for explaining the magnetic property of the respective ferrite is chosen. It is seen form Table1 that the lattice constant values match well with the experimental one. The distribution of cations in A- and B-site for all the concentrations of La substituted Mg-Zn ferrite system is given in table.1. It is known that La^{3+} ions have high octahedral preference energy and therefore replaces Fe^{3+} ion of comparatively smaller radius present in B-site. The increased substitution of La^{3+} ions in B-site pushes Fe^{3+} ions of smaller radius into A-site.

3.2.2 FAR-IR Study

The Far-IR spectra of $Mg_{0.5}Zn_{0.5}La_xFe_{2-x}O_4$ have been studied in the frequency range 200-600cm^{-1} and it is shown in Fig.4. All the spectra except x = 0.0 showing four prominent absorption bands among which two main bands are strong (υ_1 and υ_2) while the other two (υ_3 and υ_4) exhibit weak absorption.

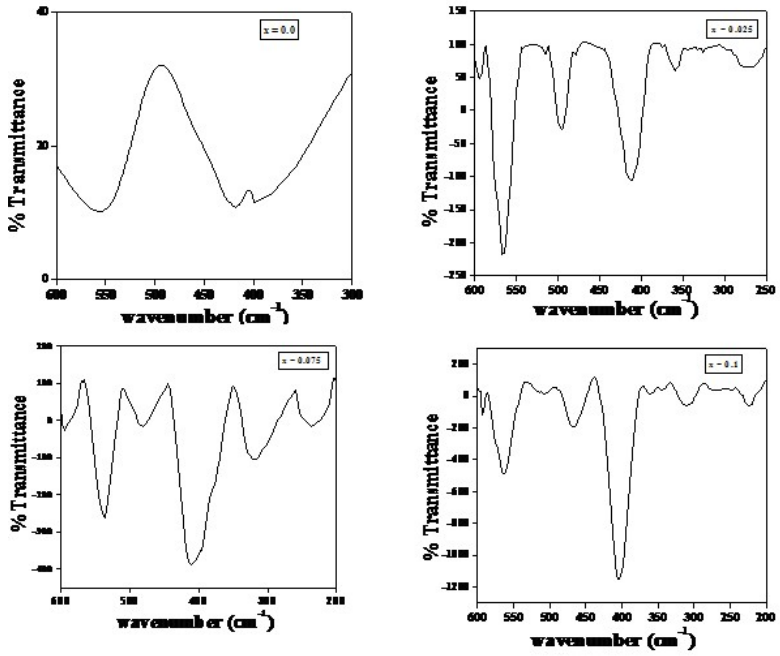

Fig.4 Far-IR spectra of $Mg_{0.5}Zn_{0.5}La_xFe_{2-x}O_4$

Waldron [16] based on a potential energy study attributed the band around 600 -500 cm^{-1} to the vibration of ions in the tetrahedral site and that around 500-400 cm^{-1} to the vibration of ions in the octahedral site. In the present study of $Mg_{0.5}Zn_{0.5}La_xFe_{2-x}O_4$, tetrahedral vibrations are found to be in the range 564-550 cm^{-1}. The main octahedral vibrations are found to be in the frequency range 463-495 cm^{-1} with an additional vibration mode at 409-433 cm^{-1}. The resolved Far-IR spectra illustrates the existence of shoulders in A- and B-sites for the samples x=0.025 to x=0.1. The sample x = 0.0 displays a single band for A-site and two bands for B-site vibrations. The presence of shoulders in B-site indicates the existence of excessive Fe^{2+} ions which cause local lattice deformation due to the Jahn-Teller effect in Fe^{2+}. This leads to a non-cubic component in the crystal field potential and to the splitting of the bands [17-18].

Table 2: Absorption frequency data of $Mg_{0.5}Zn_{0.5}La_xFe_{2-x}O_4$

Concentration X	Frequency data of absorption bands (cm^{-1})			
	υ_1	υ_2	υ_3	υ_4
0.0	560	435	391	391
0.025	560,593	495,411	359	278
0.05	537,593	488,443	382	302
0.075	541,593	479,410	319	229
0.1	563,593	463,405	313	222

The data of absorption frequency of $Mg_{0.5}Zn_{0.5}La_xFe_{2-x}O_4$ system is presented in table.2. It is seen from table 2 that the octahedral bands show a shift to lower frequencies with La substitution. It explains that the substituted La has replaced Fe^{3+} ion in B-site due to its larger ionic radius and relatively greater mass than the other constituent. The replaced Fe^{3+} ion migrates to A-site which is evident from the cation distribution. It is also seen that the value of tetrahedral band frequency υ_1 increases with La concentration. The increase in values is interpreted as follows: It can be recalled that the solubility limit of La in B-site is up to x = 0.025, after which excess La ion diffuses out of the B-site and forms a secondary phase with the displaced Fe^{3+} ion in A-site and tend to reside along the grain boundaries. This causes appreciable contraction of A-site and hence tends to increase the value of υ_1. It is also seen that the intensity of shoulder in A-site increases with the La concentration with its peak position unaltered which suggests that La has occupied A-site after reaching the solubility limit in B-site. The third vibrational band υ_3 corresponds to vibration of metal ion –oxygen complexes in octahedral site and their band positions are found to be dependent on the masses of Mg^{2+},$Zn^{2+}$and Fe^{2+} ions in B-site. The fourth vibration band υ_4 in the range 391-222cm^{-1} is very weak and

corresponds to lattice vibrations [19-22] due to tetrahedral metal- ion complexes. Thus it follows that the Far-IR method has proved itself handy in explaining the cation occupancies in the present ferrites.

3.3 Morphological Analysis

The SEM micrographs of nano $Mg_{0.5}Zn_{0.5}La_xFe_{2-x}O_4$ are shown in Fig.5. It is difficult to decide the accurate grain size from the SEM micrographs as they don't focus distinct grain boundaries. However they reveal that the constituent structures are agglomeration of particles. The agglomerations have sizes of the order of several hundreds of nanometers. Thus the grains obtained by the present method of synthesis are comparatively in nano sizes. The dark portions in micrographs indicate the holes left out by the gases released during the synthesis.

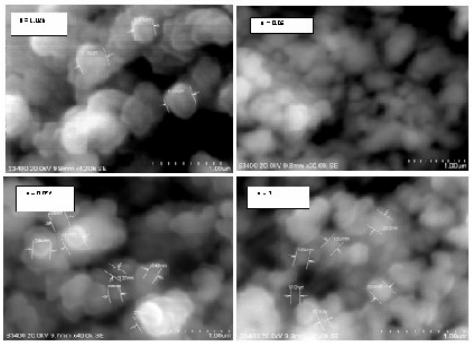

Fig.5: Surface morphology of Mg $_{0.5}$ Zn $_{0.5}$ La$_{2-X}$ O$_4$ with various X

The elemental composition of the samples has been measured using energy dispersive X-ray analysis and confirmed that there are no appreciable impurities present in the prepared material. Fig.6 shows a representative EDAX spectrum of La doped Mg-Zn ferrite.

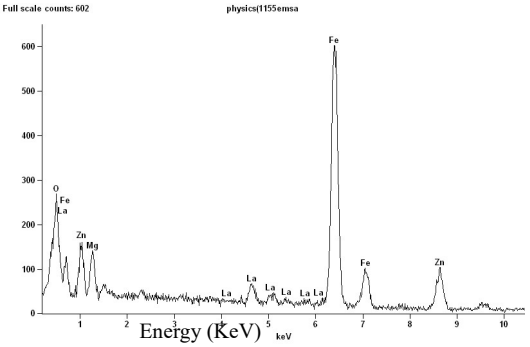

Fig.6 EDAX spectrum of La doped Mg-Zn ferrite

Further the ratio of the elements present in the samples was found to be in agreement with the chemical formula for the respective compositions. Hence the present method of synthesis has yielded reasonably pure mixed ferrites with good stoichiometry.

3.4 Magnetic Study

3.4.1 VSM Study

Magnetic hysteresis loops of nano $Mg_{0.5}Zn_{0.5}La_xFe_{2-x}O_4$ traced using VSM in a maximum field of 7000 Oe at room temperature are shown in Fig.7. It is seen from Fig.7 that the sample x = 0.0 shows clear saturation in a field of 5000 Oe. Those substituted with La do not saturate even in the maximum applied field. Magnetization values of the samples at 7000 Oe are given in table .7. It is seen from table.7 that the magnetization values decrease with the substitution of La. The trend can be explained on the basis of site occupancy of the cations and the modifications brought about in the exchange effects due to the doping of Lanthanum. The main contribution of magnetic properties derives from Fe^{3+} on B-sites of cubic spinal. The Lanthanum ion has high octahedral preference and hence occupies B-site at the expense of Fe^{3+} ion moving to the A-site. Since the magnetic moment of doped La is very small $0\,\mu_B$ compared to that of the Fe^{3+} ion $5\,\mu_B$, the magnetization of the B-sub lattice gets diluted resulting in the observed decrease in saturation magnetization for the La-substituted ferrites. It is noted that the saturation magnetization reduces abruptly with the substitution of La up to x = 0.025 but for x > 0.025 the change is gradual. This confirms that the La has reached its solubility limit after x = 0.025. The magnetization values are found to be greater than that reported for Sm doped Mg-Zn ferrite [23]. It is seen from the coercivity data that substitution of lanthanum has increased the coercivity. It is worthy to recall that the grain size had decreased with La substitution in XRD study. The variation of coercivity with grain size is explained by Stoner-Wohlfarth theory [24]. According to the theory, the coercivity is influenced by factors such as magneto crystalline anisotropy, micro strain, magnetic particle morphology, size distribution, anisotropy, and magnetic domain size.

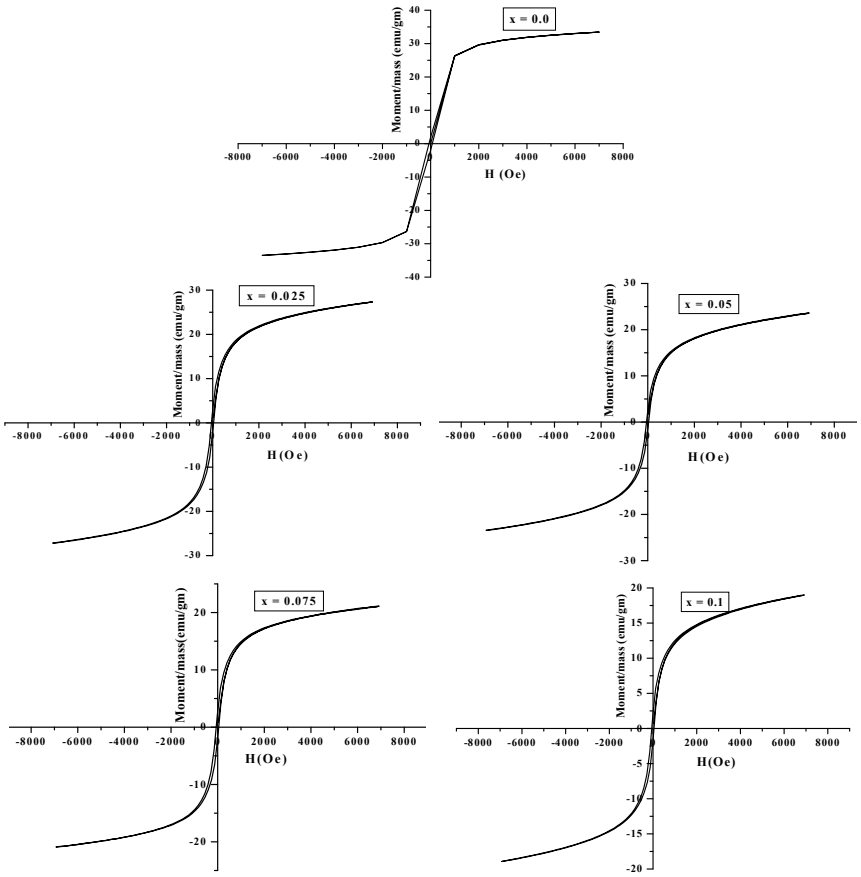

Fig.7: Hysteresis loops of nano $Mg_{0.5}Zn_{0.5}La_xFe_{2-x}O_4$ at 300K

It is known that the grain boundary increases with a decrease in crystallite size. In addition to that the presence of the secondary phase in the mist of grains of proposed ferrite may destroy the homogeneous composition. Thus hindrance to the domain wall motion occurs as the varying sizes of particles different compositions are present. This explains the increase in coercivity with increasing La content.

Table: 3: Magnetic parameters of nano $Mg_{0.5}Zn_{0.5}La_xFe_{2-x}O_4$ obtained from VSM

Concentration (x)	Magnetization M (emu/g)	Coercivity (G)	Retentivity (emu/g)	Magnetic moment (μ_B)		Canting angle (α_{YK})
				Exp	Theo	
0.0	34	45	2.748	1.432	1.245	62.4°
0.025	27	48	2.54	1.072	1.049	63.8 °
0.05	24	52	2.456	1.001	1.021	64.5 °
0.075	22	57	1.847	0.808	0.988	65.5 °
0.1	20	60	1.508	0.734	0.868	66.2 °

Spin canting is another dominant factor which plays a significant role in determining the magnetization in nano ferrites [25]. The spin canting angle obtained by applying the Yaffet-Kittel triangular lattice model to the present system is given in table 3. The theoretical moments calculated after incorporating the canting angle are found to agree with the experimental magnetic moment. This is valid since it has been already proved that the inclusion of non-magnetic ion in one sub lattice may result in the non-collinear arrangement on the other [26]. There are a few reports available in literature for magnetic study of La doped Mg-Zn ferrite. Perhaps this is the first work with a complete study on the same.

4. Conclusion

This work presents our attempt to synthesize nanoparticles of La doped Mg-Zn ferrites for microwave applications. As far as our knowledge goes there are few reports on the above material. This work, we claim as the

first on the structural and magnetic study of La doped Mg-Zn ferrites. The ferrite system of the present study has been prepared by means of the most dependable sol-gel (citrate-nitrate) route for nanoparticles. Structural and morphological studies are done using XRD, FAR-IR and SEM-EDAX instruments. The XRD studies show the formation of single phase La-doped Mg-Zn ferrite up to a concentration of x = 0.025 after which a secondary phase corresponding to $LaFeO_3$ crops up. But a gradual annealing of the as-prepared ferrites at 600^{o}C tends to reduce the intensity of the secondary phases in them. Cation distribution which has been proposed here serves as a main key to explain the structural and magnetic properties of the ferrites. FAR-IR studies, perhaps the first one on the above material gives clear picture of the formation of ferrite structures and stands a proof for the validity of the proposed cation distribution. Morphological study using SEM reveals that the particle possesses uniformity in structure along with agglomeration to some extent. EDAX analysis confirms the purity and the stoichiometry composition of the ferrites. Thermal studies on the dried gel precursor indicate the role played by La in phase formation. The study also presents various overlapped transitions that are a bit difficult to resolve form the DSC curves. Magnetic parameters obtained using VSM have been found to have a close correlation to the cation distribution. The addition of La has reduced the magnetization values where the coercivity increases making the La doped ferrites more reliable for memory storage devices. The presence of spin canting further widens the application of Mg-Zn ferrite when doped with La.

Acknowledgement

The author thank to The Central Instrumentation Facility, Pondicherry University and DST-FIST, Government of India for funding the facilities utilized in the present work.

References

1. Mangalaraja, R.V., S. Ananthakumar, P. Manohar and F.D. Gnanam, J. Magn. Magn. Mater. 253, (2002), p. 56.
2. H. Montiel, G. Alvarez, M.P. Gutiérrez, R. Zamorano and R. Valenzuela, J. Alloys Compd. 369, (2004), p. 141.
3. A.C.F.M. Costa, E. Tortella, M.R. Morelli and R.H.G.A. Kiminami, J. Magn. Magn Mater 256, (2003) p. 174.
4. L.Neel, Annls. Phys. 3, (1948) 137.
5. J.L. Snoek, New developments in ferrimagnetic materials, Elsevier Publ. Co. New York 1947.
6. R.H.Kodama, J. Magn. Magn Mater.200, (1999) 359.
7. H.H. Hamed, J.C. Ho, S.A. Oliver, R.J. Willey, G. Olivieri and G. Busca, J. Appl. Phys. 81, (1997) 1851.
8. Xu Feng, Jiang Jing, Zhou Xiangchun, Li Liangchao and Liu Hui, J. Rare earths. 25, (2007) 232.
9. Kanwar Singh Nalwa and Ashish Garg, J. Appl. Phys. 103, (2008) 044101.
10. Derek Craik, "Magnetism", Wiley Pub.1995.
11. Xiangchun Zhou, Jing Jiang, Liangchao Li and Feng Xu, J.Magn.Magn.Mater. 314, (2007) 7.
12. L. Zhao, H. Yang, L. Yu, X. Zhao, W. Sun, Y. Cui, Y. Yu and S. Feng, Phys. Stat. Sol. A 201, (2004) 3121.
13. CRC Handbook of Chemistry and Physics, E-version, 2005.
14. Liangchao Li, Hui Liu, Yuping Wang, Jing Jiang and Feng Xu, J. Colloid and Interface Science. 321, No. 2 (2008)265.
15. G.M. Bhongale, D.K. Kulkarni and V.B. Sapre, Bull. Mater. Sci. 15, (1992) 121.
16. R.D.Waldron, Phys.Rev. 99, No.6 (1955) 1727.
17. T.T.Srinivasan, C.M.Srivastava, N.Venkataramani and M.J.Patni, Bull.Mater.Sci. 6, No.6 (1984)1063.
18. K. Mohan, Y. C. Venudhar, J. Mater. Sci Lett.18, (1999) 13
19. O. S. Josyulu and J. Sobhanadri, Phys. Stat. Sol. (a) 65, (1981) 479.
20. V. R. K. Murthy, S. Chitrashankar, K. V.Reddy and J. Sobhanadri, Indian J. Pure Appl. Phys. 16, (1978) 79.
21. C. M. Srivastava, M. T. Patni and C. Srinivasan, J. Appl. Phys. 53, (1982) 2107.
22. Chang Sun, Kangning Sun, Solid.State.Commun. 141, (2007) 258.
23. E. Melagiriyappa and H.S. Jayanna, J Alloys and Compounds 482, (2009) 147.
24. Q Chen , Z Zhang J. Appl. Phys. Lett. 73, (1998) 3156.
25. R.H. Kodama, J. Magn. Magn. Mater. 200, (1999) 359.
26. J.Smit, H.P.J. Wijn, Ferrites, Cleaver-Hume Press, London, vol. 16, (1959).
27. C.M. Srivastava, M.J. Patni, J. Magn. Res.15, (1974) 359.
28. C.M. Srivastava and M.J. Patni, J. Magn. Res. 15, (1974) 359.
29. E. Schlomann, Proceedings of the Conference of Magnetism and Magnetic Materials AIEE Spec. Publ. T-91, (1956) 600.
30. E. Schlomann, J. Phys. Chem. Solids 6, (1958) 257.
31. V.K. Sankaranarayanan and N.S. Gajbhiye J. Magn. Magn . Mater 92, (1990) 217.